Biochimica et Biophysica Acta, 1057 (1991) 195–207

ADONIS 000527289100091J

BBABIO 43346

Effect of irradiance level on distribution of chlorophylls between PS II and PS I as determined from optical cross-sections

Nancy L. Greenbaum and David Mauzerall

The Rockefeller University, New York, NY (U.S.A.)

(Received 13 July 1990)
(Revised manuscript received 2 November 1990)

Key words: Photosynthetic unit; Photosystem; Reaction center; Optical cross section; Chlorophyll; Antenna; (*Chlorella*)

The number of antenna chlorophyll molecules transferring the energy of absorbed photons to the reaction center of either photosystem (PS) II or PS I (i.e., the 'size' of the PS), the numbers of RCII and I, and the Chl *b*/*a* ratio vary with growth irradiance level to optimize the efficiency of energy harvesting and utilization. The effects of photoadaptation on structural organization are best studied by methods measuring size-dependent properties in vivo. The effective optical cross-section, σ, or area available for photon capture, determined from the light-saturation characteristics of PS-specific signals following single-turnover flashes, provides this information. In these experiments, σ of PS II was calculated from the light-saturation of O_2 evolution, and that of PS I from the amplitude of a post-illumination respiratory oscillation. Cells grown under different irradiance levels were probed at wavelengths where both Chl *a* + *b* or only Chl *a* absorb. RC stoichiometries, Chl *b*/*a* ratios, and the in vivo absorption σ per chlorophyll were also measured. At all wavelengths studied, cross sections of both PS II and PS I were fit to a single size; deviation from Poissonian curves in regions of strong absorption were the result of absorption of actinic radiation within a single cell and not of heterogeneity of PS size. The yield of O_2 evolution following flashes at 723 nm was within 10% of that at shorter wavelengths. Photoadaptation to high light resulted in a greater decrease in the number of RCI than of RCII and in a decreased Chl *b*/*a* ratio in PS II. For all irradiance levels, the sum of the number of RC's times the number of chlorophylls per PS for PS II and PS I equals (±15%) the total extractable Chl/cell; therefore, to our knowledge for the first time, and by optical means, all chlorophyll can be assigned to the two photosystems.

Introduction

The concept of a photosynthetic unit, as originated by Emerson and Arnold [1], referred to the number of light-absorbing pigments contributing to formation of a photosynthetic product, oxygen. With discovery of two discrete reaction centers (RC) in eukaryotic photosynthetic organisms [2], one leading to O_2 evolution and the other donating reducing equivalents to carbon fixation, interest developed in the functional and structural distribution of light-gathering pigments between them. It is well documented that the amount of chlorophyll (Chl) and number of RC's per cell [3,4], as well as the ratio of RCII/RCI [5,6], vary in different environmental conditions, making necessary the direct measurements of the 'size' of each photosystem (PS), i.e., the number of chlorophylls contributing the energy of absorbed photons to that RC. Methods which measure properties dependent upon the size of the PS II and PS I antennae in intact, photosynthetically-competent systems are most useful (for a review, see Ref. 7), since they avoid changes which may occur upon disruption of cells. Such a method is that of measurement of the optical cross-section, σ: the area available for photon capture at a given wavelength obtained from the single turnover flash light-saturation behavior of photosystem-specific products or signals. From the fit of the data to Poissonian curves predicted by the cumulative one-hit target assumption, we gain information about antenna size and whether this size is unique. In the case of PS II, the optical cross section has been measured by the pulsed light-saturation of oxygen evolution [8–10]. A recent approach to the measurement of the cross section of PS I in vivo has utilized the light-saturation of the magnitude of a light-induced inhibition of respi-

Correspondence: N.L. Greenbaum, The Rockefeller University, 1230 York Avenue, New York, NY 10021, U.S.A.

ration to dark-adapted cells which is associated with PS I + PS II activity [10,11].

The antenna chlorophyll of higher plants and green algae is associated with chlorophyll binding proteins [12,13] which transfer energy individually or collectively to the RC. Adaptation by the organism to different light intensities during growth alters amounts of specific components, resulting in changing Chl *b/a* ratios [8,14] as well as total chlorophyll per RC [6,8,9] and RC per cell [5,7,15]. Because Chl *a* and b have partially overlapping absorption spectra, measurements of the optical cross-section made at wavelengths where one chlorophyll absorbs more than the other provide information concerning how Chl *a* and *b* are partitioned between the two photosystems.

From the studies described here, we have drawn several conclusions about the inherent absorption properties of the two photosystems and composition of their antennae in *Chlorella*: (1) the optical cross-section of PS II is, at all wavelengths studied, indicative of a single (or narrow distribution in) size; deviation from the fit to a Poissonian curve at wavelengths of strong absorption is the result of absorption of the actinic radiation in the algal cell and not of heterogeneity in the size of the photosystem; (2) the optical cross-section of PS I, measured by the amplitude of the respiratory oscillation in the presence of the PS II inhibitor DCMU, is also fit by a single Poissonian curve; in absence of the inhibitor, this signal is the sum of contributions from both photosystems; (3) contrary to the generally held view that the yield of oxygen production drops at wavelengths greater than 690 nm, the same amount (within 10%) of oxygen is formed per flash at 723 nm as at shorter wavelengths, but with a much smaller optical cross-section; (4) for cells grown under varying irradiance, the greatest changes occur in the amount of Chl *b* and therefore in the size of PS II, and in the number of PS I; (5) the sum of the number of RC's multiplied by the number of chlorophylls per unit for PS I and PS II accounts for the total amount of extractable chlorophyll ($\pm 15\%$) per cell.

Materials and Methods

Algal cell growth conditions. Batch cultures of the green alga *Chlorella vulgaris* were grown at 20 °C in Burr's medium on a rotary shaker or were magnetically stirred. Cells referred to in the text as 'intermediate' and 'low' light-grown cells were illuminated by cool-white fluorescent bulbs at approx. 133 and 2.5 μE m^{-2} s^{-1}, respectively (Model QSL-100 light meter, Biospherical Instruments, San Diego, CA), and 'high' light-grown cells were illuminated by a metalarc lamp at approx. 8300 μE m^{-2} s^{-1}. Cells grown in intermediate and high light doubled approx. every 24 and 12 h, respectively. 3–4-day-old cells were collected from exponentially growing cultures of high and intermediate light-grown cells (low light-grown cells were approx. 20 days old when harvested) by centrifugation, and were resuspended in the same buffer plus 1 mM $NaHCO_3$. Growth conditions, with some variation in growth intensities, are similar to those used previously [8,10]. Cell counts were made in duplicate with a hemocytometer. Chlorophyll concentrations were determined by absorbance at 647 and 664.5 nm in 80% acetone extracts of the cells according to the equations of Inskeep and Bloom [16].

Emerson-Arnold numbers. Rates of O_2 production by cell suspensions in response to flashing light were measured in a closed lucite chamber with a Clark-type electrode. Three synchronously triggered xenon flashlamps (Stroboslave type 1539A) surrounding the chamber provided saturating flashes at a frequency of 20 flashes/s. The width of the flashes was 1.6 μs and 7.5 μs at one-half and one-tenth maximal intensity, respectively.

Measurement of RCII and RCI stoichiometries. The total Chl/RCII was calculated by dividing the Emerson-Arnold number by 4 (the assumed number of light-driven one-electron oxidation steps required to oxidize water to molecular oxygen). The concentration of P700, the primary electron donor of RCI, was calculated from the light-induced absorbance change at 720 minus 697 nm in the presence of ascorbate and methylviologen, using an extinction coefficient of 64 mM^{-1} cm^{-1} (Ref. 17; measurements made at Brookhaven National Laboratories according to Refs. 5,15). To aid in the disruption of the cell wall for this measurement, cells were first treated as for the carboxyatractyloside-inhibition studies (see ahead) then sonicated in 50 mM Tris buffer (pH 7.6) with 0.05% Triton X-100.

Measurement of the optical cross-section per pigment. The absorption spectra of cell suspensions were measured with an Aminco-Chance DW-2A spectrometer. The effects of light scattering were effectively cancelled by use of the technique of Shibata et al. [18]: a highly scattering white filter, composed of three layers of opalescent plastic film (backing of 'Lettraset' press-on letters), was inserted between the cuvettes (both sample and reference) and photomultiplier. Spectra between 350 and 800 nm were recorded for several dilutions of the cell suspension. Linearity of plots of cell concentration vs. absorbance for various wavelengths, and extrapolation of each plotted line through the origin, verified that light-scattering effects had been cancelled. The apparent absorptions and the measured number of chlorophyll molecules in the sample were used to calculate the effective optical cross-section per Chl in vivo, using the conversion factor: cross-section ($Å^2$ per molecule) = decadic molar extinction coefficient (M^{-1} cm^{-1}) $\times (3.82 \cdot 10^{-5})$.

Optical cross-sections of PS II and PS I. Relative O_2 flash yields (measure of PS II activity) and respiratory oscillations (correlated with PS I activity) were measured with a Pickett-type O_2 polarograph according to previously described methods [8,10]. Based upon the known diameter of a *Chlorella* cell of approx. 4 μm, the settled cells were calculated to cover 30–40% of the platinum electrode surface (i.e., less than a monolayer of cells).

Microsecond light pulses were provided by a Candela LFDL-2 flashlamp-pumped dye laser, using dye solutions of 70 μM rhodamine 6G/0.1% lauryldimethylamine oxide in 60% MeOH (maximum emission, 588 $\pm$ 2.5 nm), 40 μM sulforhodamine 640 in MeOH (maximum emission, 655 $\pm$ 1.5 nm), 120 μM LD700 in MeOH (maximum emission, 723 nm), or 40 μM oxazine 720 in MeOH (maximum emission, 695 $\pm$ 2.5 nm). All dyes were obtained from Exciton. Wavelengths of maximal output and bandwidths were measured by a Jarrel Ash (Waltham, MA) model 82-410 monochromator. The laser flash was delivered to the electrode unit via one arm of a bifurcated fiber-optic light-pipe, the exit of which was fixed 8 mm above the electrode surface. The laser light leaving the light-pipe was observed to illuminate the electrode surface uniformly. The energy of each flash reaching the aperture of the fiber optic was attenuated by a Newport model 135-5 attenuator (Fountain Valley, CA) and insertion of calibrated filters of various concentrations of Cr-, Ni-, Co- and $CuSO_4$ contained in closed glass cuvettes (5 cm diameter $\times$ 2.0 or 2.5 cm light path). The absolute flash energy for each attenuation reaching the electrode surface was determined in separate measurements by inserting the end of the fiber optic into a pulsed light detector (Laser Precision Corp. model RJP 734 plus Rj-7200 Energy Ratiometer; Utica, NY) or bolometer (Scientech Model 360203 Laser Power Meter) which were cross-calibrated (agreement within 5%). The amount of light reflecting from the electrode surface was measured to be 70% of incident light intensity in the absence of cells and approx. 30% in the presence of cells at the strongly absorbed wavelength of 655 nm. Some scatter occurs at the electrode surface because it is not perfectly smooth. Therefore, since cells received the reflection of up to 70% of the photons not absorbed on the first pass, it was estimated that a total of 1.5-times the fluence exiting from the fiber optic was incident upon the cells; this correction was included in calculation of total light energy. Because of variations in the absorption by cells with different amounts of pigmentation or slightly different cell density, as well as variations in absorption of light of different wavelengths, the factor of 1.5 can only be considered an approximation. We estimate that the actual amount of light received may vary as much as 5% from this value for different experiments. The energy of each flash before attenuation was monitored by a thin glass beam-splitter and an Eppley thermopile. The output of the thermopile was amplified and recorded on the second channel of the recorder used for the O_2 measurements.

Light-saturation curves of O_2 production were measured according to the method of Ley and Mauzerall [8]. In the presence of dim background white light (2 μE m^{-2} s^{-1}, roughly 1% of the intensity required to saturate photosynthesis) through the second arm of the fiber optic to randomize S-states, cells received a series of laser flashes at a frequency of approx. 0.4 Hz. Cells were pulsed by saturating flashes (10^{15}–10^{17} Q cm^{-2}, depending upon the wavelength) until a steady-state amount of O_2 was formed in response to each flash, after which the laser flash was attenuated. Oxygen evolution as the result of the first attenuated flash was recorded. The light-saturation curve was generated by alternating saturating and flashes variously attenuated over about 4 orders of magnitude of intensity.

Measurement of PS I activity of the peak to peak amplitude of the respiratory oscillation was carried out as in Ref. 10. Cells were dark-adapted for 3 min, after which they received a series of laser flashes of varied energy, usually 8 at the rate of 6/s. O_2 evolution occurred (starting with the third flash), followed by the respiratory oscillation, which occurred in the dark after a several-second lag and on a minute time scale (Fig. 5A). In some experiments 3 μM DCMU in dimethylsulfoxide (DMSO; 0.1% final volume – DMSO alone had no effect) was added. In the presence of the inhibitor (Fig. 5B), there was no O_2 evolution, but the oscillation persisted (beginning several seconds after the light pulses), at 80–100% of the amplitude without DCMU. The amplitude of the oscillation was linear with the number of flashes up to at least eight flashes with DCMU and at least 15 pulses without DCMU. O_2 yields and amplitudes of the respiratory oscillation following subsaturating flashes were normalized to values following saturating flashes (repeated at frequent intervals during each experiment) and were plotted as the relative amplitude of each signal.

Inhibition of the respiratory oscillation by carboxyatractyloside. Chlorella cells were rendered permeable to carboxyatractyloside, a specific, noncompetitive inhibitor of the mitochondrial adenine nucleotide translocase [19], by preincubation with 50 mM Tris/1 mM dithiothreitol/10 mM EDTA (pH 8.0) followed by incubation for 3 h at 37 °C with Novozym 234 (10 mg/ml per 10^7 cells; gift of M. Fasullo) in buffer + 1 M sorbitol as osmoticum. Permeability was verified by osmotic swelling of cells in hypotonic buffer. Permeabilized cells were then centrifuged and resuspended in fresh buffer two times before mounting on the oxygen electrode. After verification that cells subjected to this treatment evolved oxygen and exhibited the same respiratory oscillation as did untreated cells, a single dose of 10

TABLE I

Chlorophyll and reaction centers in Chlorella

The stoichiometries of RCII and RCI in the table are the means of 4–6 determinations for each of duplicate samples from a single batch of cells grown in high (approx. 8300 μE m^{-2} s^{-1}), intermediate (approx. 133 μE m^{-2} s^{-1}), and low (approx. 2.5 μE m^{-2} s^{-1}) light. Measurements were made according to procedures described in Materials and Methods.

Growth light:	High	Intermediate	Low
Chl b/a	0.1 ± 0.04	0.27 ± 0.02	0.37 ± 0.02
$a+b$/cell ($\times 10^{16}$ mol)	1.50	5.85 ± 0.70	8.45
Chl/O_2 (Emerson-Arnold number)	1360	3980	4484
RCII/cell ($\times 10^{-5}$)	2.7	3.5	4.5
RCI/cell ($\times 10^{-5}$)	3.3	7.5	4.9
RCII/RCI	0.80	0.47	0.93
$a+b$/cell via Eqn. 1: RCII $\times \sigma O_2$ + RCI $\times \sigma$I ($\times 10^{16}$ mol)	1.61	6.10	8.60

mM carboxyatractyloside in buffer was added to the buffer circulating directly over the cells.

Inhibition of the respiratory oscillation was also achieved by inclusion of glucose or acetate to the circulating buffer (Fig. 5C).

Results

For each set of growth conditions (high, intermediate, and low growth irradiances), measurements were made of the optical cross-sections for oxygen production and the respiratory oscillation (in the presence and absence of DCMU), and optical cross section per absorbing pigment in vivo. Wavelengths were chosen at which Chl *a* and *b* had either similar (e.g., 588 or 655 nm) or very different (695 or 723 nm) absorption. Measurements were also made of the Chl b/a ratio, the number of Chl $a+b$ per cell, the stoichiometry of RCII and RCI, and the Emerson-Arnold number (Chl/O_2 formed per single turnover flash) for each set of conditions.

Stoichiometric measurements

Cells grown under different light regimes had Chl b/a ratios ranging from 0.1, in high light, to 0.4, in low light (Table I). As in previous studies in *Chlorella* [8,9], the Emerson-Arnold number varied over a 5-fold range for cells grown in low light (5000 ± 500) to high light (1200 ± 200), with intermediate light-grown cells having 3400 ± 500 Chl per oxygen molecule per flash. The RCII and RCI stoichiometries listed in Table I were used for calculation of the distribution of total chlorophyll (see below). The measurements reported are the mean of 4–6 determinations for each of duplicate samples from a single batch of cells grown under each irradiance level, and were performed during the same time period as the measurement of the optical cross-sections. An identical set of stoichiometric measurements was repeated at a later date. While there were small variations in absolute values consistent with a decrease in growth irradiance level in the second set of measurements, all values were internally consistent and relationships among the values remained similar to those from the first set of measurements. The Emerson-Arnold number divided by 4, and then by the total extracted Chl $a+b$ per cell, yielded the approximate number of RCII per cell: $2.66 \cdot 10^5$, $3.54 \cdot 10^5$ and $4.54 \cdot 10^5$ RCII in cells grown in high, intermediate and low light, respectively. From the light-induced absorbance change at 697 nm, $3.33 \cdot 10^5$, $7.48 \cdot 10^5$ and $4.88 \cdot 10^5$ RCI were calculated to be present in the same cells. As seen under a microscope, cells grown under extreme low light were considerably smaller than the other cells; therefore fewer RC/cell were not indicative of lesser density of photosynthetic apparatus.

The optical cross-section of a chlorophyll molecule in vivo

Because of the effects of heterogeneous absorption and light-scattering, the optical cross-section of pigments in vivo is not likely to be the same as in solution, particularly in regions of strong absorption. It is therefore necessary to measure the true absorption of the cell suspension with instrumental corrections for scattered light. The number of Chl $a+b$ molecules was then determined by extraction into an appropriate solvent (see Materials and Methods). In vivo optical cross-sections were calculated from the apparent absorption coefficients for each experiment (Table II). This method ignores small differences in different protein-pigment complexes and cannot be used in the 'tail' region of the spectrum, e.g., 723 nm.

At 588 nm, a region of low absorption, the mean σ(Chl $a+b$) for intermediate light-grown cells (Chl $b/a = 0.27$) was 0.33 Å^2. This value was 60% higher in high light-grown cells (Chl $b/a = 0.1$) and 20% lower in low light-grown cells (Chl $b/a = 0.4$). This variation with growth irradiance is contrary to the report by Ley and Mauzerall [8] of similar optical cross-sections of Chl $a+b$ for cells grown under all conditions at this wavelength. This may be partially due to use of the current technique for cancellation of the effects of light scattering, which has permitted more precise determination of the cross-section in regions of low absorption: the previous plots of cell dilution vs. absorbance at this wavelength did not always extrapolate to the origin. Also, the *Chlorella* cells used in these experiments have been grown under more extreme light conditions (Chl b/a as low as 0.06) than those in the previous report (Ref. 8; Chl $b/a = 0.15$), which may enhance variations. The data for $\sigma(a+b)$ vs. Chl b/a ratio can be fit by any ratio of $\sigma(b)/\sigma(a)$ between 0.1 and 1 but not > 1.

TABLE II

Optical cross-sections and absolute sizes of photosystems in Chlorella

This table summarizes the mean values for optical cross-sections per absorbing pigment (σ(Chl)) and for PS II and PS I, and the calculated number of chlorophylls per photosystem, determined by techniques described in Materials and Methods. For simplicity, the standard deviations for σ of each PS have been omitted and the number of pigments per PS have been rounded off; see text of Results for complete details. Determination of the number of chlorophylls per photosystem for measurements made at 588 and 655 nm was made with the approximation that $\sigma(Chl\ a) = \sigma(Chl\ b)$ at these wavelengths. Calculation of the number of Chl *a* per PS was based upon the observation that only Chl *a* absorbs at 695 nm and that $\sigma(a+b)$ at 655 nm $= \sigma(a)$ at 695 nm; the number of Chl *b* was calculated as Chl$(a+b)$ − Chl *a*. It should be noted that variability in measurements of σ of PS II and PS I (5–15%) implies a similar variability in the precision in the determination of the number of chlorophylls per PS.

Wavelength	σ_{chl} (Å^2)	σ_{O2} (Å^2)	σ_{OSC} (Å^2) + DCMU	Chl/PS II		Chl/PS I	
				a + *b*	*b*, *a*	*a* + *b*	*b*, *a*
High light, λ_{max} 678.5; Abs. susp./soln. 0.94							
588	0.55 ± 0.02	–	–	–		–	
655	0.99 ± 0.02	100	210	100		210	
					75*b*		25*b*
695	0.97 ± 0.07	25	180		25*a*		190*a*
Intermediate light, λ_{max} 681; Abs. susp./soln. 0.70							
588	0.33 ± 0.04	110	115	335		350	
655	0.85 ± 0.09	275	285	330		340	
					270*b*		0*b*
695	0.85 ± 0.04	55	305		60*a*		350*a*
723	(0.05)	2	17	–		–	
Low light, λ_{max} 681; Abs. susp./soln. 0.65							
588	0.25 ± 0.04	–	–	–		–	
655	0.75 ± 0.04	425	400	570		540	
					485*b*		0*b*
695	0.71 ± 0.08	60	400		80*a*		560*a*

Thus the individual σ for Chl *a* and Chl *b* are not well determined by these data. It is possible that other pigments which are present only in cells grown in very high light contribute at this wavelength. Together with low chlorophyll content in these cells, absorption by these pigments may confuse the measurements. However, for cells grown in intermediate irradiance, those which were used for measurements of σ for PS II and PS I in this study, our values for the σ per pigment are similar to those of Ley and Mauzerall [8].

Both Chl *a* and *b* absorb at 655 nm, which is at the peak of Chl *b* absorption. At this wavelength, as at 588 nm, the mean $\sigma(a+b)$ increased with decreased Chl *b*/*a* ratio (i.e., was largest in high light-grown cells). 695 nm is in a region of strong Chl *a* absorption with virtually no Chl *b* contribution. Similar to measurements made at 655 and 588 nm, the σ(Chl) at this wavelength is greatest in high light-grown cells, which have the lowest chlorophyll content. The data suggest that the decreased apparent absorption in the more highly pigmented cells is at least partially the result of heterogeneous absorption effects in cells with higher chlorophyll content [20,21]. A shift in the maximal absorption peak of chlorophyll is observed, from 682 nm in low and intermediate light-grown cells to 678 nm in high light-grown cells. This shift is consistent with evidence for varying amounts of different Chl-binding proteins with different spectral properties under different growth conditions [13,14,22]. Further analysis of the changes in the pigment cross-sections with light adaptation depend on quantitative spectral characterizations of the individual pigment proteins, i.e., cross-sections or extinction coefficients – information which is not yet available. 723 nm is far out on the 'tail' of Chl *a* absorption, where only a fraction of chlorophyll molecules may be absorbing; therefore, the total chlorophyll cannot be used to determine a useful σ(Chl) at 723 nm.

Optical cross-sections of PS II and PS I at 588 nm

Flash energies at the oxygen electrode surface were varied over 4 orders of magnitude, from 10^{12}–10^{16} quanta/cm^2 per flash. Similar to previous reports [8,10,11], the data can be fit by the cumulative one-hit saturation function, or Poisson distribution ($Y = Y_0(1 - e^{-\sigma E})$, where Y is the yield of O_2 per hit). Using the saturation amplitude Y_0 and the cross-section $\sigma(O_2)$ as adjustable parameters, the flash intensity data were fit by an iterative non-linear least squares fitting program. The $\sigma(O_2)$ corresponding to the best fit for the 'size' of the PS II target (RC + antenna Chl) absorbing photons at this wavelength was 111 ± 6 Å^2 (Fig. 1). This size is approx. 30% larger than the size of PS II reported by Ley and Mauzerall [8] for 'intermediate' light-grown cells. This difference appears to be the result of slightly

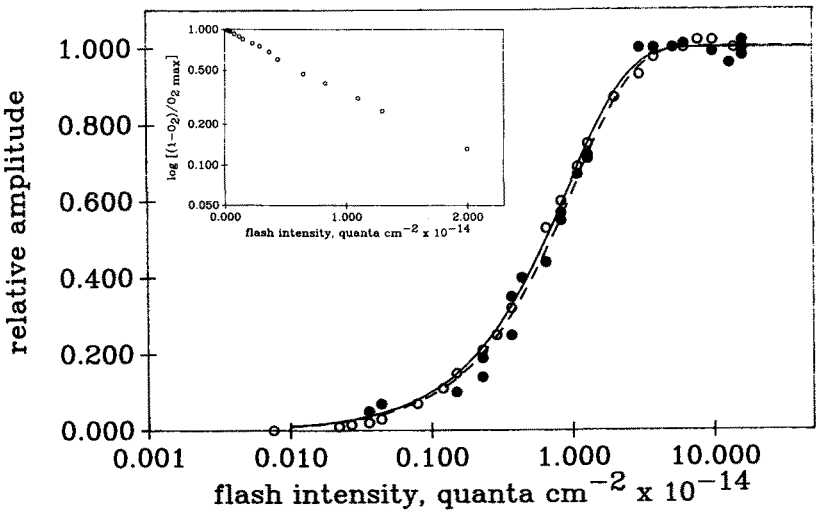

Fig. 1. Light-saturation behavior of the amplitude of O_2 flash yields (○) and respiratory oscillation (●) in *Chlorella* grown under intermediate light (see Materials and Methods) at 588 nm. The solid curve fit to the O_2 flash yield data is the cumulative one-hit saturation function calculated for a unique mean $\sigma = 107 \pm 2$ Å^2. The dashed curve fit to the oscillation data is the function calculated for a $\sigma = 97 \pm 4$ Å^2. The inset figure is a 'killing curve' plotted from the O_2 data.

lower growth irradiance in the present experiments, as the Emerson-Arnold number and Chl/cell for these cells are also proportionally larger than in the earlier report. A plot of $\ln(1 - O_2$ yield$/O_{2\max})$ vs. intensity ('killing curve'; inset of Fig. 1) yields a straight line. Linearity of this plot, in agreement with the fit of the Poissonian curve, is consistent with former determinations of homogeneity in the size of PS II units [8,11].

The light saturation of the respiratory oscillation at 588 nm was fit with a single Poissonian with a cross-section similar to that of PS II, 116 ± 26 Å^2 (Table II). The degree of scatter in the data did not permit differentiation between a fit by a single Poissonian or the sum of two with a small (less than 2-fold) difference in size. Although there was no oxygen production in the presence of DCMU, the respiratory oscillation persisted with little or no decrease in the amplitude at saturating flash energies. The shape and σ of the curve in the presence of DCMU was not significantly different from that measured in its absence.

Optical cross-sections at 655 nm

The σ at 655 nm for oxygen production in cells grown in intermediate light, 277 ± 34 Å^2, was more than twice that measured at 588 nm, 111 Å^2. Unlike the measurements at 588 nm, however, the light-saturation

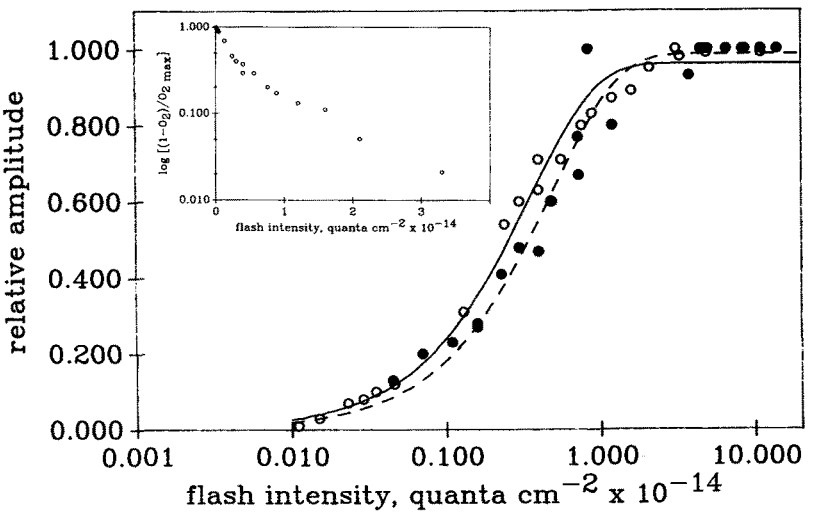

Fig. 2. Light-saturation behavior of O_2 flash yields (○) and respiratory oscillation (●) of intermediate light-grown *Chlorella* cells at 655 nm. The curve fit to the O_2 yields (———) has a unique $\sigma = 286 \pm 16$ Å^2, and that to the respiratory oscillation (- - - - -) has $\sigma = 204 \pm 14$ Å^2. A 'killing curve' of the same data is shown in the inset.

behavior in the region of the curve approaching saturation deviated from the Poissonian curve (Fig. 2). A 'killing curve' plotted from the same data (inset of Fig. 2) demonstrated an apparent biphasicity. Such behavior is consistent either with heterogeneity in the size of PS II or with effects of inhomogeneous actinic light caused by absorption in a single cell at a highly absorbing wavelength. This effect was less pronounced in cells grown in high light ($\sigma = 98 \pm 12$ Å^2), which have less Chl *b* ($0.3 \cdot 10^{-16}$ mol/cell, compared with $2 \cdot 10^{-16}$ mol/cell in intermediate light grown cells), 25% fewer PS II, and smaller antennae (Ref. 8; this report), and was more visible in the more highly pigmented cells grown in low light ($\sigma = 426 \pm 37$ Å^2; $4 \cdot 10^{-16}$ mol Chl *b*/cell) (data not shown).

The light saturation curve for the respiratory oscillation for intermediate light-grown cells at 655 nm was also fit by a single Poissonian, with a cross-section of 204 ± 14 Å^2. With the addition of DCMU (Fig. 2), the curve still had a Poissonian shape and a cross section of 287 ± 14 Å^2. The cross-section of PS I of low light-grown cells, 400 ± 13 Å^2, was not significantly different from that of PS II in the same cells (426 ± 25 Å^2). In the high light-grown cells, however, the σ of the respiratory oscillation, 210 ± 15 Å^2 with or without DCMU, was considerably larger than that of PS II (98 Å^2), i.e., the σ values of the two photosystems did not vary in a similar manner. Because of scatter in the data, σ of PS I could not be clearly resolved into two discrete components.

Optical cross-sections at 695 nm

The wavelength 695 nm was chosen because, although only Chl *a* absorbs there, the total absorption is the same as that at 655 nm. It was therefore possible to determine the number of Chl *a* contributing to each photosystem. Only one pigment absorbs at this wavelength, and the cross-section per pigment was observed to decrease in cells grown in less light. Therefore, it can be concluded that there is suppression of apparent absorption caused by heterogeneous absorption. As at 655 nm, the light-saturation curve deviated from the Poissonian curve in the region of near-saturating intensities, and was most pronounced in the more highly pigmented cells. In cells grown in high, intermediate, and low light, the optical cross-section was 25 ± 1, 53 ± 5 (Fig. 3) and 59 ± 3 Å^2, respectively.

The light-saturation behavior of the respiratory oscillation was, in cells grown under all conditions, very broad, and could be fit with the sum of two Poissonian curves (Fig. 3). Although the scatter of the plotted points of the respiratory oscillation was too large to achieve a unique resolution, the fit was consistent with the smaller of the two cross-sections being approximately the same size as the σ for O_2 evolution at this wavelength, and the larger cross-section being 6–10-times this size. As at the other wavelengths, there was no oxygen evolution if DCMU was included in the buffer, but the kinetics of the respiratory oscillation were unchanged and the amplitude was maintained within 80–100% of the control (uninhibited) amplitude. In the presence of the inhibitor, however, the light-saturation data were fit by a single Poissonian of 304 ± 47 Å^2, similar to the size as the large component of the broad curve generated in the absence of the inhibitor (Fig. 3 and Table II).

Optical cross-sections at 723 nm

Following saturating laser pulses at 723 nm, approximately the same amount of O_2 was formed as at other wavelengths. However, a much higher fluence was

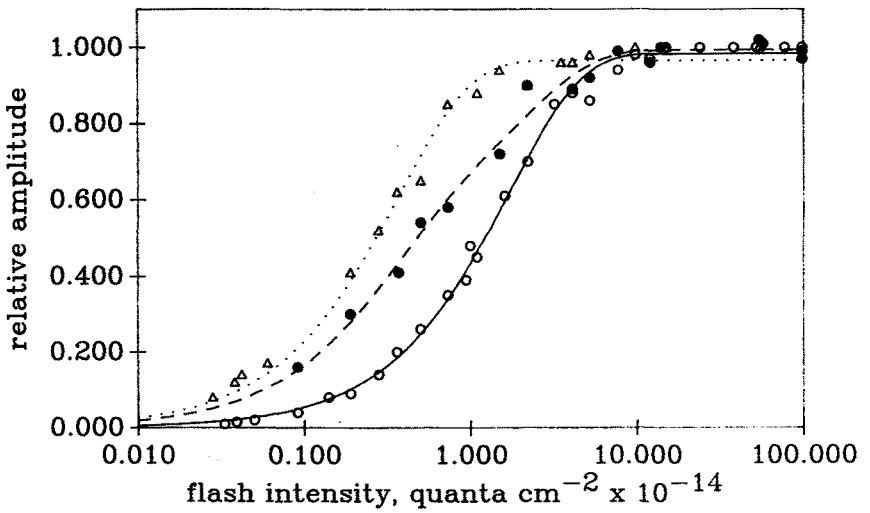

Fig. 3. Light-saturation behavior of O_2 flash yields (○) and respiratory oscillation (●, without DCMU; △, with 3 μM DCMU) in *Chlorella* grown in intermediate light at 695 nm. The data for the O_2 yield (———) and the respiratory oscillation + DCMU (· · · · · ·) are fit by curves with $\sigma = 58 \pm 2$ and 271 ± 14 Å^2, respectively. The data for light-saturation of the respiratory oscillation are fit with a curve (- - - - - -) which is the sum of equal ($\pm 12\%$) contributions of Poissonians with σ values of 346 ± 105 and 49 ± 14 Å^2.

required for saturation than at other wavelengths (10^{17} quanta cm^{-2} per flash at 723 nm, compared with 10^{15}–10^{16} for the other wavelengths at which measurements were made). The light-saturation curve for oxygen evolution is fit by a single Poissonian curve with a very small σ, 1.8 ± 0.1 Å^2 (Fig. 4).

Similar to the measurements made at 695 nm, the light-saturation curve at 723 nm for the respiratory oscillation (Fig. 4) was considerably shifted to lower intensities and was far broader than that for oxygen evolution [7,8]; the best fit was the sum of two Poissonian curves representing approximately equal contributions of σ of 2.3 ± 0.4 Å^2 (i.e., similar to that of oxygen production) and 19 ± 3 Å^2 (Fig. 4). In the presence of DCMU, oxygen evolution was inhibited and the amplitude of the oscillation at saturating light intensity was unchanged within 20%. In the presence of the inhibitor, the data were fit by a single Poissonian with a σ of 17 ± 1 Å^2 (Fig. 4), similar to that of the larger component of the broad curve in its absence.

The number of chlorophylls per photosystem and distribution of total chlorophyll

By dividing the optical cross-section of a photosystem by the cross-section per pigment at the same wavelength, the number of chlorophylls in that photosystem is calculated (see Table II). At 588 nm, if the simplifying approximation (see Discussion) is made that the optical cross-sections of Chl *a* and *b* are approx. equal, one can divide the cross-section of the photosystem by the cross-section per pigment to get the number of pigments per photosystem, in this case 336 Chl $a+b$ for PS II and 348 Chl $a+b$ for PS I. $\sigma(a+b)$ at 655 nm varies over the range of growth irradiances similarly to $\sigma(a)$ at 695 nm for the same range. Therefore, we have concluded that $\sigma(a) = \sigma(b)$ at this wavelength, and have divided the σ for each PS at 655 nm by σ(Chl) to obtain the approximate number of Chl $a+b$ per PS: 99, 326 and 568 Chl $a+b$ per PS II, and 212, 338 and 533 Chl $a+b$ per PS I in high, intermediate and low light-grown cells, respectively. The number of pigments determined in the intermediate light-grown cells by measurements at 588 and 655 nm are very similar, verifying the precision of the technique.

At 695 nm, the optical cross-section for oxygen production can be converted into the number of Chl *a* per PS II by dividing by the cross-section per pigment. For cells grown in high, intermediate and low light, there are 26, 62 and 83 Chl *a* per PS II, respectively. The cross-sections for the respiratory oscillation at this wavelength (in the presence of DCMU) were converted to PS I sizes of 189 Chl *a* in high light, 357 Chl *a* in intermediate light and 563 Chl *a* in the low light-grown cells.

The fraction of Chl *a* per PS can be calculated by division of the number of Chl *a* (measured at 695 nm) by the number of Chl $a+b$ (measured at 655 nm) for the same conditions. It is estimated that Chl *a* comprises the following proportions of total chlorophyll of Photosystems II and I in each group of cells (values from Table II):

Cells	% of photosystem comprised of Chl *a*:	
	PS II	PS I
High light	26	98
Intermediate	19	106
Low light	15	106

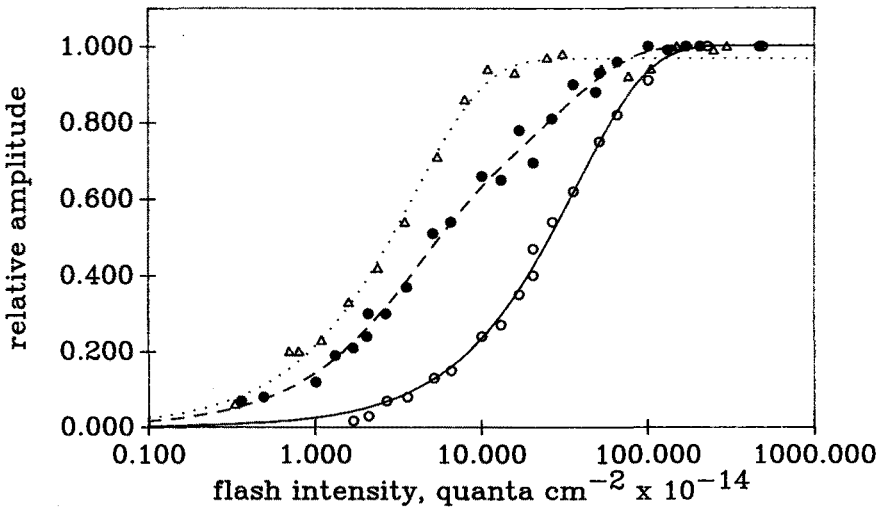

Fig. 4. Light-saturation behavior of O_2 flash yields (○) and respiratory oscillation (●, without DCMU; and △, with DCMU) of intermediate light-grown *Chlorella* at 723 nm (data from ref. 11). The curve fit to the O_2 data (———) is a Poissonian with $\sigma = 1.8 \pm 0.04$ Å^2, and that fit to the oscillation + DCMU (·····) has $\sigma = 17 \pm 1$ Å^2. The broad curve fit to the oscillation (- - - - -) is the sum of equal (±5%) contributions of Poissonians with $\sigma = 19 \pm 3$ Å^2 and 2.3 ± 0.4 Å^2.

There is little or no Chl *b* in PS I, and the Chl *b/a* ratio in PS II ranged from approx. 3 in high light grown cells to 6 in low light cells. The variability in measurement of the sizes of the photosystems (Table II) was less than 10% for PS II, but approached 15% for PS I; precision in the calculation of the distribution of Chl *a* and *b* between the photosystems is therefore within these limits.

From the number of RCII and RCI per cell and the number of antenna chlorophylls associated with each unit, one can determine if all measured chlorophyll can be accounted for by the following expression:

$$\text{total Chl} = [N(\text{II}) \cdot n(\text{II})] + [N(\text{I}) \cdot n(\text{I})] \quad (1)$$

where n is the number of RC and N is the number of antenna pigments associated with that RC. From measurements where both Chl *a* and *b* absorb (588 and 655 nm), there is good agreement between the calculated total chlorophyll (sum of the products of number and size of the two units, taken from data in Tables I and II) and that measured by extraction for all sets of growth conditions. In evaluating the total Chl calculated from Eqn. 1, precision of the measurements is limited by the variability in all the measurements (5–15%).

Cells	Chl/cell (extraction) ($\times 10^{16}$ mol)	Chl/cell from eqn. 1 ($\times 10^{16}$ mol)	% in PS II $N(\text{II}) \cdot n(\text{II})$	% in PS I $N(\text{I}) \cdot n(\text{I})$
High light	1.50	1.6	27%	73%
Intermediate	5.85	6.1	31%	69%
Low light	8.45	8.6	50%	50%

Low light-grown cells have an approx. equal distribution of total Chl between the two photosystems, but with increasing growth irradiance, proportionally more of the chlorophyll is associated with PS I. 'Inactive' or 'precursor' RCII's [23–25] not evolving oxygen do not contribute to this RCII measurement; however, there is no pool of excess chlorophyll which is not associated with RCII or RCI.

By substitution of values for Chl *a* from experiments at 695 nm into Eqn. 1, the distribution of Chl *a* between the two photosystems can be evaluated:

Cells (% *a*)	Chl *a*/cell (extracted) ($\times 10^{16}$ mol)	Chl *a*/cell from Eqn. 1 ($\times 10^{16}$ mol)	% of the cell's Chl *a* in:	
			PS II	PS I
High light (91)	1.37	1.2	10%	90%
Intermediate (79)	4.62	4.8	8%	92%
Low light (73)	6.17	5.2	12%	88%

There is little variation in the fractional distribution of Chl *a* between the photosystems in cells grown under different conditions. Therefore, the increased Chl *b/a* ratio in cells grown at lower light levels is indicative of increased Chl *b* deposition in PS II. Again, by the above calculations, the sum of measured values agrees closely with the amount of Chl *a* extracted. For high light-grown cells, however, $[N_a(\text{II}) \cdot n(\text{II})] + [N_a(\text{I}) \cdot n(\text{I})]$ for Chl *a* is approx. 20% less than the total extracted chlorophyll Chl *a*.

Carboxyatractyloside inhibition of the respiratory oscillation

Cells rendered osmotically sensitive by incubation with proteolytic enzymes were placed upon the oxygen electrode as in the other experiments. These cells were competent for oxygen formation and the respiratory oscillation following laser flashes. Following addition of carboxyatractyloside or atractyloside, oxygen formation persisted, yet the respiratory oscillation was inhibited (data not shown). As there is no protein analogous to the mitochondrial adenine nucleotide translocase in the chloroplast membrane [19], the respiratory oscillation must be of mitochondrial origin.

Similarly, the respiratory oscillation, but not oxygen evolution, was inhibited by inclusion of 1 mM acetate in the circulating buffer (Fig. 5C).

Discussion

Origin of the respiratory oscillation

Observations by Ried [26,27] led to his assignment of the respiratory oscillation as a PS-I-mediated inhibition of cellular respiration. This conclusion was based upon approximate adherence to published action spectra [28] and inhibition of oxygen evolution and the subsequent oscillation by different compounds [26]. Alternatively, similar O_2 transients have been attributed to oscillations in the rate of O_2 evolution following changes in illumination [29–31]. We consider the latter interpretation untenable, as oxygen is formed within 2 ms after flashes [32–35] and the subsequent oscillations occur in the dark, following a delay of several seconds, for several minutes after O_2 evolution has ceased [10,26,27]. The two processes can be readily resolved in Fig. 5, and are independently inhibited (oxygen evolution by DCMU, the respiratory oscillation by millimolar concentrations of glucose [26] or acetate. This process is also distinct from chlororespiration [36,37] or the inhibition of chlororespiration [38]: the time-scales are different. Experiments on *Chlorella* by Peltier and Ravenel [37] and by Peltier et al. [38], which have been reproduced in this laboratory in *Chlorella* and in isolated spinach chloroplasts (Greenbaum, N.L., unpublished data), have shown 'chlororespiratory' activity to occur on a < 1 s time-scale), and the respiratory oscillation does not occur in isolated spinach chloroplasts (i.e., whole cells are required). These data, combined with the inhibition of the respiratory oscillation by carboxyatractyloside, support the hypothesis that the oscilla-

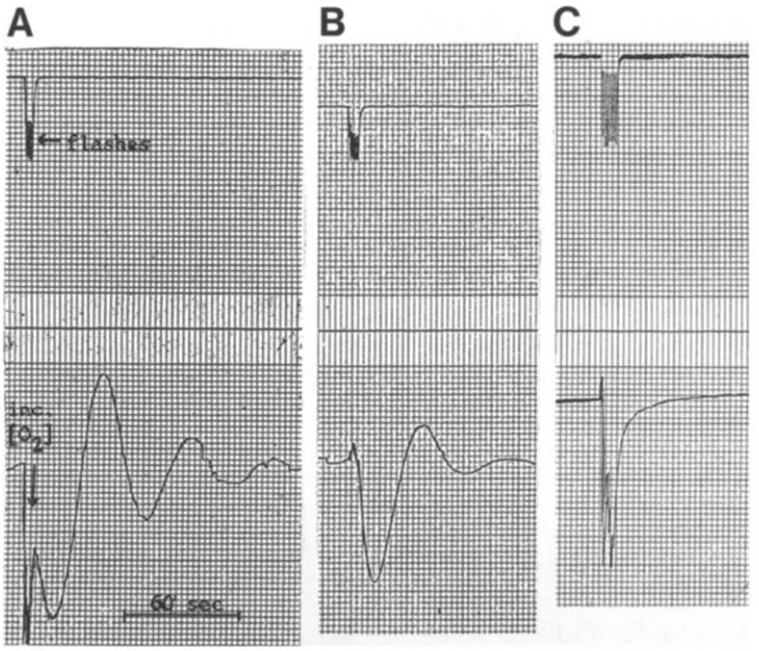

Fig. 5. Time-course of oxygen evolution and respiratory oscillation following laser flashes. The upper trace records the output of the thermopile used to monitor the total energies of eight flashes before attenuation. The lower trace shows the output of the oxygen detection circuit. The baseline represents the rate of O_2 uptake in the dark. *Chlorella* cells were dark-adapted for 3 min before laser flashes. (A) Oxygen evolution, followed by respiratory oscillation upon return to dark. (B) Respiratory oscillation only in the presence of the PS II inhibitor DCMU. The absolute amplitude of the oscillation following saturating flashes was the same (within 20%) in the presence or absence of DCMU. (C) Oxygen evolution, but no respiratory oscillation, in the presence of 1 mM acetate.

tion represents a transient inhibition of mitochondrial respiration in response to chloroplast-generated ATP (transported across the chloroplast membrane in the form of triosephosphates and subsequently oxidized in the cytosol [39] prior to the light-activation of ATP-requiring key enzymes of the carbon fixation cycle [40]). Preliminary data from this laboratory, as well as those of other authors under similar conditions [41,42], indicate that time-resolved changes in the cytosolic concentrations of ATP and ADP follow the pattern predicted by this model: a decreased rate of respiration was associated with increased cytosolic [ATP] and decreased [ADP] and vice versa.

Contributions of both photosystems to the respiratory oscillation

The light-saturation behavior of the respiratory oscillation at both 723 and 695 nm was best fit by the sum of approximately equal contributions of two Poissonians, one a size similar to that for O_2 production and one roughly ten times that size. The broad curve was originally assigned to contributions from two discrete populations of PS I to the overall signal [11]. However, if this interpretation were correct, addition of DCMU to inhibit electron transfer from PS II would not influence the light-saturation plot of the oscillation. This is not the case, however, as inclusion of the inhibitor results in a light-saturation curve which is fit by a single Poissonian approximately equivalent in size to the larger of the two cross-sections resolved from the broad curve in the absence of the inhibitor. It therefore appears that the oscillation is the result of contributions from both photosystems, and that the broad curve is the summation of both cross-sections and the ratio of their contributions.

At wavelengths where the cross-sections of PS II and PS I are similar to each other (e.g., 588 or 655 nm), addition of DCMU made no visible difference in the shape of the curve of the respiratory oscillation. It is of interest to note that the amplitude of the oscillation in the presence of the inhibitor following saturating flashes is not significantly diminished from that of the oscillation in its absence. Such a decrease in the presence of DCMU would be expected if the amplitude of the oscillation were dependent upon the summed contributions of linear electron flow from both photosystems. If the hypothesis is correct that the oscillation is the result of a transient ATP-mediated inhibition of mitochondrial respiration, then in the absence of electron transport from PS II, ATP levels maintained by cyclic phosphorylation in PS I could sustain the activity responsible for this signal [43]. Recent observations of thermodynamic efficiency of photosynthesis in *Chlorella* determined by pulsed photoacoustic calorimetry has shown the efficiency to increase, or at least remain constant, when DCMU is present [44]. These observations support the postulate that cyclic PS I activity increases the efficiency of energy storage in the presence of DCMU.

Therefore, the light-saturation curve of the respiratory oscillation can be resolved into components which appear to be contributions from both PS II and PS I, and the composite curve represents a simultaneous measurement of the optical cross-sections of both photosystems.

Effect of light adaptation on PS size and distribution of Chl a and b

The use of optical cross-sections in determination of the size of photosynthetic units offers distinct advantages [7,8]. Perturbation of the physiological system is minimal, and measurements are rapid enough to prevent changes within the time course of the experiment. Under favorable conditions, this approach permits noninvasive measurement of both PS I and PS II in photosynthetically active cells under identical conditions. It is well documented that oxygen evolution is a linear measure of PS II activity, and the amplitude of the respiratory oscillation has also been demonstrated to be linear with the number of light pulses in the absence or presence of DCMU. Therefore, particularly by use of probing wavelengths at which both Chl $a+b$ or only Chl a absorb, it has been possible to determine not only the total number of chlorophylls, but also the distribution of Chl a and b per PS in cells grown at different irradiance levels. It can be seen in Table II that lower growth irradiance resulted in larger antenna sizes of both PS II and PS I. However, the extent of the changes of each PS are not parallel (Table II): the size of PS II varied over nearly a 6-fold range (from 100 to 570 Chl $a+b$), while that of PS I varied over a 2.5-fold range (from 210 to 530 Chl $a+b$).

Varied growth irradiance also results in an altered Chl b/a ratio because of the larger increase in PS II which has a greater fraction of Chl b (Table II). Similar numbers of chlorophylls per PS I determined from measurements made at 695 and 655 nm indicate that, in all cells examined, the PS I antenna is composed almost entirely of Chl a, in agreement with the values in the literature for isolated reaction centers with antenna proteins [14].

Chlorophyll activity

By use of Eqn 1, it is also possible to determine whether we can account for all the chlorophyll in a cell. In intermediate light-grown cells, the number of units times the total chlorophyll per unit for PS I and PS II approximately equals the total extracted chlorophyll (within 5%). A similar relationship holds for low light-grown cells. Only in the high light-grown cells is there somewhat less agreement: the amount of Chl a extracted from high light-grown cells is 20% greater than the sum calculated from the cross-sections. In these high light-grown cells, the chlorophyll absorption peak was observed to shift from 681 nm (in low- and intermediate light-grown cells) to 678.5 nm. Different absorption spectra have been measured for various Chl a/b binding proteins from spinach [22] and from maize [13], some of which absorb far less at 695 nm than others. If a similar range occurs in the absorption of the Chl proteins of *Chlorella*, and there are relatively more of the shorter wavelength-absorbing proteins in the high light-grown cells (consistent with the observed blue-shift of the pigment spectrum in these cells), it is possible that the measured absorption at 695 nm does not include all the chlorophyll, and that our estimation of the σ(Chl) at 695 nm may be slightly underestimated. There is also evidence from action spectra for special forms of Chl a [45]. Ley had measured a minimum PS II size of 21 Å^2 at 592 nm [9], which he translated into 75 Chl/PS II, and had assumed this to approach the RC core size (Chl a only). However, comparison of the present results at 695 nm (Chl a only) with those at 655 nm (Chl $a+b$) in high light-grown cells indicates that Chl b comprises up to 75% of the photosystem. As quantitative data (in cross-sections or extinction coefficients) of the pigment protein complexes become available, a better analysis of the pigment distribution in the photosystems, including specific complexes, will be possible.

Oxygen production at 723 nm

Although O_2 evolution as far in the red region as 747 nm has been observed [46], the belief has remained that the efficiency is low [28]. The data in Fig. 4 clearly demonstrate, however, that not only can oxygen be made by 723 nm light, but that it follows the same light-saturation behavior and has the same yield (within 10%) as at the other, more conventional PS II wavelengths (< 670 nm). It is simply that the effective optical cross-section is much smaller. It is important to note, however, that this part of the absorption spectrum is on the 'tail' of Chl a absorption, and is therefore not representative of the average Chl a absorption, i.e., it may well consist of only a particular fraction of the total chlorophyll. Our calculations of PSU size in terms of molecules assume a constant photochemical yield of trapping in a reaction center following excitation, i.e., the measured apparent cross-section is the true cross-section times this yield [7]. Since we are not certain of the molecular cross-section of a possibly special Chl a at 723 nm, we cannot check if this yield is constant. An estimate of σ(Chl) at 723 nm can be made from the fact that the number of Chl a in PS I is known (from 695 nm) and using this number, together with the σ of PS I at 723 nm in intermediate light-grown *Chlorella*, 17 Å^2, one calculates a cross-section of 0.05 Å^2 per Chl a.

Absorption by optically thick samples

Light-saturation curves of oxygen flash yields from spectral regions of low absorption (e.g., 588 or 723 nm) are fit by Poissonian curves predicted by cumulative one-hit target theory. Similar plots from measurements

made in regions of intense absorption, such as 655 or 695 nm, however, deviate from the Poissonian curve in the part of the curve approaching saturation. Replotted as so-called 'killing curves', the same data demonstrate a clear nonlinearity at 655 and 695 nm and are linear at 588 and 723 nm. Such effects can be the result of optical thickness of the sample on the electrode surface, inhomogeneous illumination of the sample, discrete populations of optical cross-sections contributing to the signal, or inhomogeneous actinic illumination in a single cell at a highly absorbing wavelength. Frequent observation of the uniformity of illumination exiting the fiber optic light pipe, and use of less than a monolayer of cells on the electrode surface exclude the first two possibilities. Biphasicity in plots of laser flash-induced oxygen production at 674 nm in experiments of Boichenko and Litvin [47] have been interpreted as heterogeneity in PS II by these authors. It is our opinion that heterogeneous actinic light absorption within a single cell causes the apparent biphasicity in the 'killing curve' and apparent smaller absorption cross-section in the log plots of these authors. Such an effect would be maximized at wavelengths of high absorption and at high concentration of chromophore in non-random systems (such as chloroplasts). Therefore, in regions of low absorption (e.g., at 588 or 723 nm), the cell or chloroplast is closer to being optically thin. This is not the case in regions of strong absorption (655 or 695 nm) in our experiments or those of Boichenko and Litvin, particularly in the more highly pigmented *Chlorella* cells grown in low light regimes or in isolated spinach chloroplasts (data not shown). Conversely, the effect is less in high light-grown *Chlorella* and essentially absent in *Synechococcus lividus* (cyanobacterial cells which are smaller than green algae and in which the light-harvesting complexes are more evenly distributed in the thylakoid membrane than the stacking in algal chloroplasts; Greenbaum, N.L., unpublished observations). Additionally, the optical cross-section per pigment for wavelengths of intense absorption is less in the more highly pigmented samples; this observation cannot be simply the result of altered Chl *b/a* ratios in the various cell growth conditions, as it also occurs when probed at wavelengths where only Chl *a* absorbs. It therefore reflects the heterogeneous light absorption effect maximal at high absorption. In agreement with this analysis, the more recent work of Boichenko and Litvin [48] shows only one cross-section for O_2 production. However, they claim that PS I, measured by H_2 production by anaerobic *Chlorella*, is heterogeneous. We see such a broad light saturation curve only when there is electron transport through both photosystems (in the absence of DCMU) under conditions with different σ for PS II and PS I (such as at 695 or 723 nm).

We have computed the effect of internal attenuation of actinic light on the pulsed saturation curves of Figs. 2 and 3. The biphasicity can be explained by a large attenuation at 655 and 695 nm in highly pigmented cells. The attenuation required for this fit, however, may be exaggerated by internal scattering in the cell or chloroplast. Thus, while this explanation is consistent with the data, it is not possible to draw quantitative conclusions because of the complexity of light absorption in a heterogeneous, scattering, optically thick sample.

The effects of heterogeneous absorption in non-random systems in regions of intense absorption are generally treated by use of a calculated 'flattening factor', based upon the measurements by Duysens [20] and by Pulles [49]. This correction, which can amount to more than 50% of the measured absorption, is defined by the authors as the ratio of the absorption of the extracted chlorophyll divided by the absorption of the cell suspension containing equal amounts of chlorophyll. For a given set of experimental conditions, the appropriate value is chosen from an empirically-derived table. There is a large range of values for the ratio associated with different growth irradiances, as well as large standard deviations in the more pigmented cells, neither of which is addressed in the application of a generalized flattening factor. In the present experiments, we have approached the problem from the other, simpler direction: instead of applying an empirically determined correction which necessarily implies assumptions for a specific system, we have directly measured the effective optical cross-section per pigment in vivo, i.e., under the same conditions as the cross-section of the photosystem was measured. Therefore, both pigment σ's and photosystem σ's within a single cell are subjected to the same degree of 'flattening' effects and internal scatter and other index of refraction effects, and no approximations or assumptions are required in the determination of pigments per photosystem.

Acknowledgements

The authors wish to thank Kevin Wyman and Paul Falkowski for the determinations of P700 made at Brookhaven National Marine Biological Laboratory, Tim Marinetti for assistance with the curve-fitting program, and Zvy Dubinsky for helpful discussions. Comments and suggestions made by the reviewers were also appreciated. This research was supported by NSF grant DMB 87-18078.

References

1 Emerson, R. and Arnold, W. (1932) J. Gen. Physiol. 16, 191–205.
2 Kok, B. (1956) Biochim. Biophys. Acta 22, 399–401.
3 Dubinsky, Z., Falkowski, P.G. and Wyman, K. (1986) Plant Cell Physiol. 27, 1335–1349.
4 Kawamura, M., Mimura, M. and Fujita, Y. (1979) Plant Cell Physiol. 20, 697–705.

5 Falkowski, P.G., Owens, T.G., Ley, A.C. and Mauzerall, D.C. (1981) Plant Physiol. 68, 969–973.
6 Neale, P.J. and Melis, A. (1986) J. Phycol. 22, 531–538.
7 Mauzerall, D. and Greenbaum, N.L. (1989) Biochim. Biophys. Acta 974, 119–140.
8 Ley, A.C. and Mauzerall, D. (1982) Biochim. Biophys. Acta 680, 95–106.
9 Ley, A.C. (1986) in Photosynthesis Research, Vol. 10, pp. 189–196, Martinus Nijhoff, Dordrecht.
10 Greenbaum, N.L., Ley, A.C. and Mauzerall, D.C. (1987) Plant Physiol. 84, 879–882.
11 Greenbaum, N.L. and Mauzerall, D. (1986) in Progress in Photosynthesis Research (Biggins, J., ed.), Vol. II, pp. 65–68, Martinus Nijhoff, Dordrecht.
12 Thornber, J.P., Peter, G.F. and Nechushtai, R. (1987) Physiol. Plant. 71, 236–240.
13 Bassi, R., Høer-Hanson, G., Barbato, R., Giacometti, G.M. and Simpson, D.J. (1987) J. Biol. Chem. 262, 13333–13341.
14 Sukenik, A., Bennett, J. and Falkowski, P.G. (1988) Biochim. Biophys. Acta 932, 206–215.
15 Falkowski, P.G. and Owens, T.G. (1980) Plant Physiol. 66, 632–635.
16 Inskeep, W.P. and Bloom, P.R. (1985) Plant Physiol. 77, 483–485.
17 Hiyama, T. and Ke, B. (1972) Biochim. Biophys. Acta 267, 160–171.
18 Shibata, K., Benson, A.A. and Calvin, M. (1954) Biochim. Biophys. Acta 15, 461–470.
19 Stubbs, M. (1981) in Inhibitors of Mitochondrial Function (Erecińska, M. and Wilson, D.F., eds.), pp. 283–304, Pergamon Press, Oxford.
20 Duysens, L.N.U. and Sweers, H.E. (1963) in Studies on Microalgae and Photosynthetic Bacteria (Miyachi, S., ed.), pp. 353–372, University of Tokyo Press, Tokyo.
21 Berner, T., Dubinsky, Z., Wyman, K. and Falkowski, P.G. (1989) J. Phycol. 25, 70–78.
22 Evans, J.R. and Anderson, J.M. (1987) Biochim. Biophys. Acta 892, 75–82.
23 Melis, A. (1985) Biochim. Biophys. Acta 808, 334–342.
24 Chylla, R.A., Garab, G. and Whitmarsh, J. (1987) Biochim. Biophys. Acta 894, 562–571.
25 Graan, R. and Ort, D.R. (1986) Biochim. Biophys. Acta 852, 320–330.
26 Ried, A. (1968) Biochim. Biophys. Acta 153, 653–663.
27 Ried, A. (1969) in Progress in Photosynthesis Research, Vol. I (Metzner, H., ed.), pp. 521–530, H. Laupp, Jr., Tübingen.
28 Ried, A. (1971) in Proceedings of the 2nd International Congress on Photosynthesis, Stresa, Italy (Forti, G., Avron, M. and Melandri, A., eds.), Vol. I, pp. 763–772, Dr. W. Junk, Dordrecht.
29 Walker, D.A., Horton, P., Sivak, M.N. and Quick, W.P. (1983) Photobiochem. Photobiophys. 5, 35–39.
30 Walker, D.A., Sivak, M.N., Prinsley, R.T. and Cheesbrough, J.K. (1983) A.R.C. Research Group on Photosynthesis, University of Sheffield, Ann. Rep., pp. 1–5.
31 Stitt, M. (1986) Plant Physiol. 81, 1115–1122.
32 Joliot, P. and Joliot, A. (1968) Biochim. Biophys. Acta 153, 625–634.
33 Etienne, A.L. (1968) Biochim. Biophys. Acta 153, 895–897.
34 Sinclair, J. (1969) Biochim. Biophys. Acta 189, 60–64.
35 Mauzerall, D. (1990) Plant. Physiol. 94, 278–283.
36 Bennoun, P. (1982) Proc. Natl. Acad. Sci. USA 79, 4352–4356.
37 Ravenel, J. and Peltier, G. (1985) C.R. Acad. Sci. Paris, t. 301, 643–646.
38 Peltier, G., Ravenel, J. and Vermeglio A. (1987) Biochim. Biophys. Acta 893, 83–90.
39 Heber, U. and Heldt, H.W. (1981) Annu. Rev. Plant Physiol. 32, 139–168.
40 Bassham, J.A. and Buchanan, B.B. (1982) in Photosynthesis: Development, Carbon Metabolism, and Plant Productivity, Vol. II (Govindjee, ed.), pp. 141–189, Academic Press, New York.
41 Giersch, C., Heber, U. Kobayashi, Y., Inoue, Y., Shibata, K. and Heldt, H.W. (1980) Biochim. Biophys. Acta 590, 59–73.
42 Hampp, R., Goller, M. and Ziegler, H. (1982) Plant Physiol. 69, 448–455.
43 Arnon, D.I. and Chain, R.K. (1975) Proc. Natl. Acad. Sci. USA 74, 4961–4965.
44 Cha, J. and Mauzerall, D. (1990) 10th International Biophysics Congress, Vancouver, BC, Abs. No. P7.3.26.
45 Myers, J. and French, C.S. (1960) J. Gen. Phys. 43, 723–736.
46 Myers, J. and Graham, J.-R. (1963) Plant Physiol. 38, 105–116.
47 Boichenko, V.A. and Litvin, F.F. (1986) Dokl. Akad., Nauk. SSSR 286, 733–737.
48 Boichenko, V.A., Ladygin, V.G. and Litvin, F.F. (1989) Mol. Biol. (Moscow) 23, 107–118.
49 Pulles, M.P.J., Van Gorkom, H.J. and Verschoor, A.M. (1976) Biochim. Biophys. Acta 440, 98–106.